Temperature of mesospheric ice particles simultaneously retrieved from 850 cm^{-1} libration and 3200 cm^{-1} vibration band spectra measured by ACE-FTS

S. V. Petelina[1] and A. Y. Zasetsky[2,3]

Received 14 September 2010; revised 23 November 2010; accepted 6 December 2010; published 11 February 2011.

[1] We report a new approach to the retrieval of ice particle temperature in the atmosphere from midinfrared remote sensing observations. Two different in physical nature spectral bands of water ice, the libration band near 850 cm^{-1} and O-H stretch band at 3200 cm^{-1}, are used simultaneously. The use of both bands in the unified least squares fitting procedure enables one to enhance the stability of fitting, as well as to improve the reliability and accuracy of retrieved ice temperature values. A set of reference spectra for the least squares minimization is compiled from experimental temperature-dependent optical constants for water ice that are available in the literature. The method is applied to the observations made by the Atmospheric Chemistry Experiment Fourier Transform Spectrometer (ACE-FTS) instrument on board the SCISAT-1 satellite. According to our results, a combination of the vibration (3200 cm^{-1}) and rotation (850 cm^{-1}) bands within a unified minimization procedure can significantly, by about 4K, reduce the upper estimate of the total uncertainty in the retrieved temperatures from 12 K down to 8 K. The average temperature of bright mesospheric ice clouds observed by ACE-FTS during July 2005 is found to be about 131K, in contrast to the value of 135K retrieved from the vibration band alone.

Citation: Petelina, S. V., and A. Y. Zasetsky (2011), Temperature of mesospheric ice particles simultaneously retrieved from 850 cm^{-1} libration and 3200 cm^{-1} vibration band spectra measured by ACE-FTS, *J. Geophys. Res.*, *116*, D03304, doi:10.1029/2010JD015050.

1. Introduction

[2] Knowledge of actual temperatures of tiny ice particles that form in the upper mesosphere during the local summer, typically poleward of 50°N/S, is important for a better understanding of the physical mechanisms of ice formation and growth in such remote regions. Furthermore, it is essential for a correct interpretation of the observed variability and trends in the upper mesospheric ice layers and their attribution to the changes in neighboring environment that can be linked to modern climate change [e.g., *Thomas*, 2003; *Lübken et al.*, 2007; *Shettle et al.*, 2009]. When ice particles grow to optically visible sizes, they are referred to as polar mesospheric clouds (PMCs) or noctilucent clouds (NLCs). These clouds are composed of water ice that originally nucleates near the mesopause, at the altitudes of 87 to 91 km [e.g., *Rapp and Thomas*, 2006; *Zasetsky et al.*, 2009a], consequently grows at rates that are still poorly understood [e.g., *von Zahn and Berger*, 2003; *Murray and Jensen*, 2009; *Zasetsky et al.*, 2009b] and sediments down to 80–82 km, where it evaporates, and forms a seasonally enhanced water vapor layer [e.g., *Urban et al.*, 2007].

[3] Much effort has been put into the analyses of the upper mesospheric temperature and its relation to the observed properties of ice particles. Investigation methods range from the in situ measurements using the falling spheres technique [*Lübken*, 1999] and various ground-based lidar observations [e.g., *Hansen and von Zahn*, 1994; *Gerding et al.*, 2007] to modeling [e.g., *Rapp et al.*, 2002] and satellite-based observations that are integrated over a line of sight of 200 to 400 km in the atmosphere [e.g., *Petelina et al.*, 2005; *Hervig and Siskind*, 2006; *Hervig et al.*, 2009a]. As the technology of satellite based instruments advances further and offers a high-quality data on a nearly global scale [e.g., *Bernath et al.*, 2005; *Russell et al.*, 2009], the detection of water ice particles and their properties in the signal integrated over a horizontal optical path of 200–400 km long, particularly with respect to the temperature retrieval, is becoming possible.

[4] First retrievals of the temperature of mesospheric ice, which are independent of ice-free regions that are inevitably present along the line of sight of satellite instruments, were reported by *Petelina and Zasetsky* [2009]. The method uses infrared spectral measurements across the 3200 cm^{-1} O-H

[1]Department of Physics, La Trobe University, Melbourne, Victoria, Australia.
[2]Kurnakov Institute of General and Inorganic Chemistry, RAS, Moscow, Russia.
[3]Department of Radio and Electrical Engineering, Moscow State Technical University, Moscow, Russia.

0148-0227/11/2010JD015050

stretch band (vibrational mode) and is based on a strong temperature dependence of the ice spectrum observed by *Clapp et al.* [1995] in the study of frequency-dependent optical constants of water ice at atmospherically relevant temperatures. The ice temperature retrieval technique reported by *Petelina and Zasetsky* [2009] was developed for the solar occultation measurements of atmospheric extinction by the Atmospheric Chemistry Experiment Fourier-Transform Spectrometer (ACE-FTS). This technique was then successfully applied to the data obtained by the Solar Occultation For Ice Experiment (SOFIE) on the Aeronomy of Ice in the Mesosphere (AIM) satellite [*Hervig and Gordley*, 2010]. As shown in the abovementioned papers, the derived "true" ice temperature was, on average, 5° to 30° colder than the atmospheric temperature retrieved by the standard operational algorithms from CO_2 observations. Such difference is not unexpected because of several issues inherent to satellite remote sensing, such as very long optical paths sampled, wide fields of view, and interstitial warm regions along the optical path. We also note that near the temperature minimum of the mesopause, any vertical smoothing will tend to produce vertically averaged temperatures that are biased high with respect to the true local temperature.

[5] While the "true" temperature of mesospheric ice particles (further referred to as "ice temperature") is retrieved from the O-H stretch band measurements independently of the surrounding air temperature, its values are subject to several sources of errors: uncertainties in the range of 9 to 12K have been reported by *Hervig and Gordley* [2010] and *Petelina and Zasetsky* [2009], respectively. Moreover, it seems rather difficult to enhance the accuracy of such retrievals based on the O-H stretch spectral feature alone. One source of these uncertainties arises from a relatively low intensity of ice signal in observed infrared spectra (which translates to a low signal-to-noise ratio) due to low water content in the upper mesosphere. The other source of uncertainties is that the band shape of the O-H stretch mode also depends on the shape of ice particles, and the particle shape effect on the O-H band shape resembles, to a certain extent, the corresponding temperature effect on the extinction spectrum of ice. The difficulties are compounded by the fact that there have not yet been reported any single set, or a compilation of several consistent sets, of optical constants for water ice (and other atmospherically relevant condensed matters) over required temperature and wavelength ranges measured with the desired precision.

[6] In this work, we improve the accuracy of ice temperature retrievals by using an additional (to the O-H stretch band at 3200 cm^{-1}) spectral feature of the ice spectrum centered, at typical temperatures needed for the mesospheric ice formation, near 850 cm^{-1}. This broad spectral mode between 500 and 1000 cm^{-1} is attributed to the rotational motion of the permanent dipole moment of water molecules and is often referred to as the libration band. There are several advantages in the simultaneous use of both the O-H stretch (vibration) band and the libration band. First, the magnitude of the resonant effect, which is a primary cause of the particle shape effect on the absorption band shape, is dependent on the absolute value of the imaginary index of refraction n'' (see below). Thus the retrievals are expected to be much less affected by the shape of ice particles in the region from 400 to 1000 cm^{-1} (in which the values of n″ are at least 5 times lower than those in the O-H stretch region).

[7] Second, the reorientations of H_2O molecules responsible for absorption near 850 cm^{-1} are totally different in nature from the O-H valence vibrations responsible for the 3200 cm^{-1} band. Therefore, we are looking at two different kinetic temperatures, namely *translational temperature* of the O-H vibrations and *rotational temperature* of the water molecule librations. In other words, we simultaneously use two different physical mechanisms for the characterization of temperature of the same material and therefore expect to determine it more accurately. Moreover, due to its rotational origin, the position of the libration mode depends strongly on temperature [*Zasetsky and Gaiduk*, 2007]. In order to test its accuracy and reliability, the proposed new method is applied to the ACE-FTS PMC spectra recorded in July 2005. A more detailed description of the instrument and PMC detections is given by *Bernath et al.* [2005], *Eremenko et al.* [2005], and *Zasetsky et al.* [2009a] and will not be repeated here. The ACE-FTS parameters relevant to PMC studies are as follows. Vertical field of view is 4 km, which increases the likelihood to observe warmer (ice-free) regions together with colder (ice-rich) regions in the mesosphere. The lowest frequency for ACE-FTS spectra is 800 cm^{-1}, which does not allow one to use the entire libration band in the temperature retrievals. This low-frequency cutoff at 800 cm^{-1}, however, does not halt the use of this spectral feature as the peak position of the libration band is shifted toward higher frequencies (850 cm^{-1}) at the temperatures typical for mesospheric ice particles. In addition to these restrictions in remote sensing observations, the values of optical constants for water ice at the summer mesospheric temperatures have only been reported in the frequency range of 800 cm^{-1} and higher [*Clapp et al.*, 1995].

2. Methodology

[8] The extinction spectrum of a particle with the radius r normalized by the particle volume is computed as follows:

$$K_{ext}(\omega) = \frac{3}{4r} Q_{ext}[r, n^*(\omega)], \quad (1)$$

where $n^*(\omega) = n'(\omega) + in''(\omega)$ is the complex index of refraction, ω is the angular frequency and Q_{ext} is the extinction efficiency that can be computed using Mie theory [*Bohren and Huffman*, 1983], T-matrix [*Mishchenko and Travis*, 1998], or discrete dipole approximation (DDA) [*Purcell and Pennypacker*, 1973; B. T. Draine and P. J. Flatau, User guide for the discrete dipole approximation code DDSCAT.6.0, 2003, astro-ph/0309069, http://arxiv.org/abs/astro-ph/0309069] methods. In the present work the DDA method is used for the error estimates. For temperature retrievals we use the T-matrix method and the inversion procedure similar to that described in detail by *Zasetsky et al.* [2004], *Eremenko et al.* [2005], *Zasetsky et al.* [2007], and *Petelina and Zasetsky* [2009]. The main difference of the current inversion procedure from that described in the above papers is that the ice particle shape is also used as an adjustable parameter. Following the approach of *Hervig and Gordley* [2010], we use randomly oriented oblate spheroids where the axial ratio parameter is allowed to vary, and the T-matrix code of *Mishchenko and Travis* [1998].

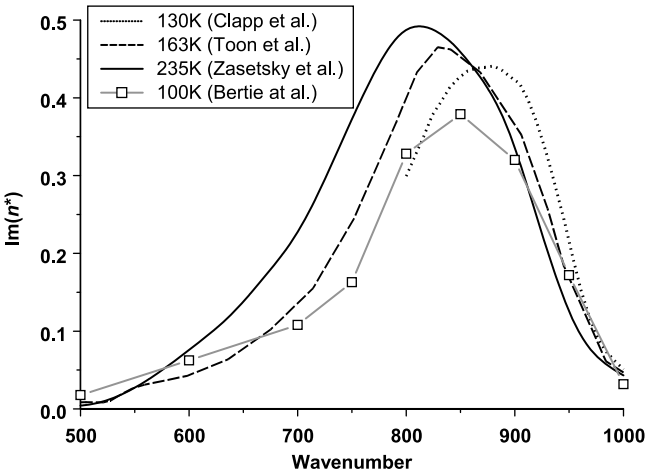

Figure 1. Temperature effect on the height and position of imaginary index of refraction for water ice in the region of 500 to 1000 cm^{-1}. Shown experimental data are: 100K [*Bertie et al.*, 1969], 130K [*Clapp et al.*, 1995], 163K [*Toon et al.*, 1994], and 235K [*Zasetsky et al.*, 2005].

[9] Optical constants of water ice in the range from 800 (the low-frequency limit for the ACE-FTS observations) to 1000 cm^{-1} and from 2800 to 3500 cm^{-1} are used in the extinction calculations. The addition of the libration mode from 800 to 1000 cm^{-1} has several advantages. First, as was mentioned in section 1, it is a rotational band and, therefore, is more sensitive to variations in temperature. This is shown in Figure 1 where the height and position of the peak in imaginary index of refraction for water ice in the region of 500 to 1000 cm^{-1} are plotted for several values of temperature typical for mesospheric conditions. Second, because of lower frequencies and lower intensities, this mode is not as strongly affected by the particle shape as the O-H stretch mode. This is illustrated in Figure 2 where this part of the spectrum, computed for spheres, spheroids, and hexagons at 130K, is shown. Therefore, addition of the libration mode to the analysis enables us to reduce uncertainties associated with the particle shape effect on the band shape of the O-H stretch mode, and thus imposes tighter constrains on the retrieved temperature values.

[10] Experimental optical constants, in particular their reliability and accuracy around the 850 cm^{-1} band, deserve an extended description. Several research groups have reported difficulties with determining these constants at frequencies below 1000 cm^{-1}. We excluded from our analysis data of *Warren* [1984] and *Warren and Brandt* [2008] measured for ambient temperatures of ~266K, and focus on the ice optical constants measured at temperatures below the temperature of homogeneous ice nucleation. *Clapp et al.* [1995] reported the discrepancy between the experimental and calculated spectra near 850 cm^{-1}, which was attributed to the truncation errors in the Kramers-Kronig integration. A similar problem was noted in the study by *Toon et al.* [1994], even though their spectral region was extended down to 500 cm^{-1}. In their work, results for imaginary index of refraction were extended to lower frequencies using the data of *Bertie et al.* [1969] in order to enhance the accuracy of Kramers-Kronig integration. Despite this effort, *Toon et al.* [1994] stated that "the value of the imaginary index of refraction derived at 500 cm^{-1} is unreliable due to the high measured transmission at that wavelength." We note that the above statement appears to be about the region with low absorbance near 500 cm^{-1}, but not around the absorption maximum at 850 cm^{-1}. As for the 850 cm^{-1} band, *Toon et al.* [1994] found substantial differences from the results of *Bertie et al.* [1969], which the authors attributed to the temperature effect.

[11] At higher temperatures of 200 and 235K, the refractive indices of ice in the frequency range from 460 to 5900 cm^{-1} were reported by *Zasetsky et al.* [2005]. In their treatment of lower frequencies by the Kramers-Kronig integration, the authors synthetically included the 200 cm^{-1} translational mode and the dielectric relaxation mode in the microwave region with the temperature-dependent parameters taken from experimental studies to reduce integration errors. In the

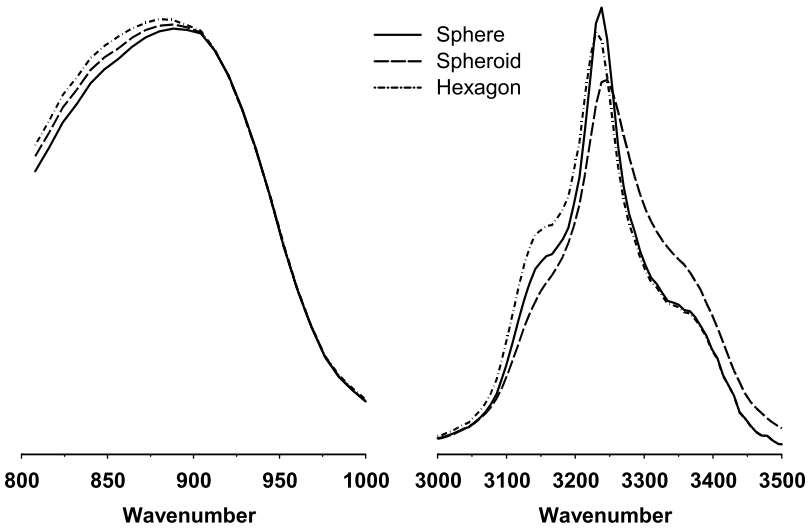

Figure 2. Simulated effect of a chosen particle shape on the ice band shape in the region (left) 800–1000 cm^{-1} and (right) 3000–3500 cm^{-1} at a temperature of 130K.

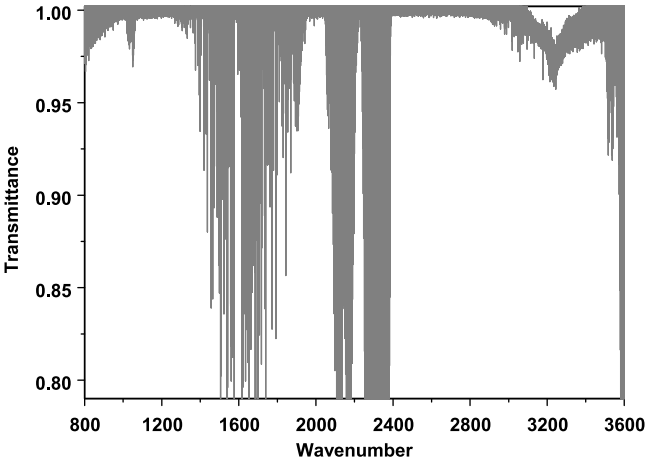

Figure 3. ACE-FTS transmission spectrum for a typical PMC with the average brightness recorded at 67.9°N and 86.9°W at an altitude of 83.8 km on 14 July 2005.

review study of optical measurements of aerosol, *Wagner et al.* [2009, Figure 10e] found that the best agreement in the atmospheric window region from 800 to 1500 cm^{-1} is achieved with the optical constants reported by *Zasetsky et al.* [2005].

[12] As mentioned before, temperature effects on the position and strength of the libration band are illustrated in Figure 1 for the following three main sets of ice optical constants: *Clapp et al.* [1995] for 130K, *Toon et al.* [1994] for 163K, and *Zasetsky et al.* [2005] for 235K. These curves are consistent in terms of variations with temperature. Note that the data of *Bertie et al.* [1969], also shown in Figure 1, appear to fall out of this sequence and, therefore, are not included in our analysis. The above three sets of optical constants show nearly linear (as a first approximation) dependencies of the peak position and its magnitude on temperature. The linear coefficients found from these three sets are -0.7 cm^{-1}/K for the position and 0.06 K^{-1} for the magnitude of the peak. Note that the temperature dependence of the peak position is about 2.5 times larger and is opposite in sign to the coefficient (0.23 cm^{-1}/K) reported by *Clapp et al.* [1995] for the O-H stretch peak, which is indicative of different physical origins of these two bands. In line with the above reasons, for the frequency range between 800 and 1000 cm^{-1} we use interpolated optical constants over the temperature interval of 235 to 120K (120K data is a linear extrapolation) obtained from the three main sets of optical constants discussed above. For the O-H vibrational mode, the original data of *Clapp et al.* [1995] in this frequency region are used.

[13] The error analysis has been carried out by a standard approach in which the total error is a combination of random and systematic errors. The estimates for random (fitting) errors are performed assuming that they are distributed normally with zero mean. The calculations based on χ^2 values give the uncertainty of about 6K for the lowest examined cloud density (0.02 $\mu m^3/cm^3$) and about 3K for the cloud with density larger than 0.08 $\mu m^3/cm^3$. It should be noted that the addition of the 850 cm^{-1} band to the analysis has resulted in the reduction of fitting error values by about 4–5K as compared to those reported by *Petelina and Zasetsky* [2009]. The systematic error, associated with the uncertainties in the experimental optical constants, is not well quantified. Possible errors in the reported optical constants are a matter of concern as spherical particle shapes were used to determine the optical constant in work by *Clapp et al.* [1995]. According to our present knowledge, the mesospheric ice particles are nonspherical and can be successfully approximated by spheroids, cubes, or hexagons [e.g., *Eremenko et al.*, 2005; *Hervig et al.*, 2009b]. No measurements were performed thus far to distinguish between the above three shapes. With a projected uncertainty of ~2 K due to the ice particle nonsphericity, which is not accounted for in the reported optical constants, the total error in the ice particle temperature retrieved in this work is estimated within the range from 5 to 8K, depending on the density of ice particles in PMCs.

3. Results and Discussion

[14] About 100 PMC observations made by ACE-FTS in July 2005 were analyzed with the described method that combines libration and vibration bands. To ensure high accuracy, only clouds with the total ice volume exceeding 0.02 $\mu m^3/cm^3$ were used for temperature retrievals. A typical ACE-FTS transmittance spectrum in the mesosphere with a prominent signature from a PMC near 3200 cm^{-1} is shown in Figure 3. As mentioned before, the lowest frequency for ACE-FTS observations is around 800 cm^{-1}. Spectral features near 800 and 3200 cm^{-1} in Figure 3 are indicative of the presence of ice particles with the size smaller than 100 nm. The presence of larger particles would have resulted in a visible scattering contribution at the high wave number end of the spectrum. However, as follows from many recent publications [e.g., *Hervig et al.*, 2009a; *Robert et al.*, 2009, and references therein], the PMC particle radii are typically smaller than 70 nm.

[15] As can be seen from Figure 3, the noise level for the ACE-FTS spectrum can be relatively high in the case of moderately bright clouds. For this reason we have applied the smoothing preprocessing using a filter based on the wavelet transforms [*Zasetsky et al.*, 2004]. As described in detail in the above work, the filtering parameters have been carefully optimized to ensure that all significant features in the ACE-FTS spectra are intact. An example of the smoothed extinction spectrum with its best fit is shown in Figure 4. It is apparent that the spectra of ice represented by randomly oriented oblate spheroids computed with the T-matrix method of *Mishchenko and Travis* [1998] fit well to the observed spectrum.

[16] The results for mesospheric ice temperatures retrieved using both the 850 cm^{-1} libration and 3200 cm^{-1} vibration bands are shown in Figure 5 by the black rhombs. The solid vertical line at about 131K indicates the mean ice temperature for these data. The temperatures retrieved for the same ACE-FTS PMC data set using the vibration band only is shown by the transparent squares, while its mean value, at about 135K, is indicated by the dashed vertical line. The standard ACE-FTS temperature (gas phase) retrieved by the operational algorithm of *Boone et al.* [2005] using a global nonlinear least squares fit to the CO_2 spectral features at 930–940 cm^{-1}, 1890–2450 cm^{-1}, and 3300–3400 cm^{-1} is shown by the gray squares. It can be seen that the gas phase retrievals yield the temperature values for PMCs that are

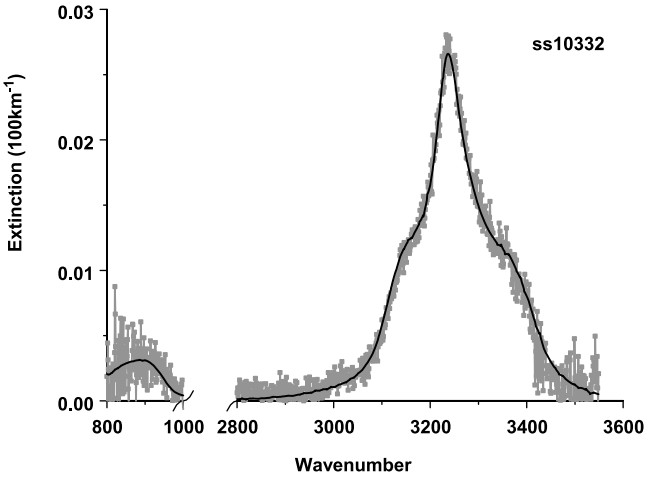

Figure 4. Typical example of the ACE-FTS PMC extinction spectrum in the 800–1000 and 2800–3500 cm^{-1} regions (gray area) together with the best fit by the computed spectrum of randomly oblate spheroids with the axial ratio of 1.9 (black curve). The spectrum (occultation number ss10332) was taken on 21 July 2005 near 67°N and 50°W at an altitude of 82 km.

sometimes higher than 150K, which is the ice freezing temperature at the lowest PMC altitudes (80–82 km). Although these gas phase temperatures are not used in the present work, we would like to comment on the occasional presence of such higher than expected values. They can be attributed to a combination of the effects of wide instrument field of view and presence of warm ice-free regions along the instrument line of sight. The first effect seems to dominate as warm biases are expected (and unavoidable) in the occultation-type observations due to large temperature gradients within the field of view. The second effect is typical for latitudes considered here (65°N–70°N) compared to higher latitudes. Also we are not aware of any systematic statistical (fitting) errors in ACE-FTS gas phase temperature retrievals that could result in them being systematically higher at mesospheric altitudes [*Sica et al.*, 2008].

[17] It should be noted that the possibility of 3–8 K temperature difference between gaseous species and ice particles in the mesosphere has been reported by *Espy and Jutta* [2002]. Such temperature difference, found from model simulations of an instant radiative heating of ice at mesopause altitudes, will likely be much lower in our case. First, most PMCs observed by ACE-FTS are located below 86 km (as the instrument is not sensitive to small particles nucleating at mesopause altitudes). Second, for medium and bright PMCs considered in this work, the temporal redistribution of the kinetic energy between particles and gas molecules should bring their *equilibrium* kinetic temperatures closer to each other.

[18] A difference between the mean ice temperature retrieved from the 3200 cm^{-1} vibration band alone (135K) and that obtained after adding the 850 cm^{-1} libration band (131K) is apparent in Figure 5. An addition of the latter band to the analysis shifts the mean ice temperature by about 4K, which is significant for mesospheric processes where even a 2K change in temperature can be very important [e.g., *von Savigny et al.*, 2007]. As described before, the uncertainty for individual data points shown in Figure 5 results from a combination of several random uncertainties and, in the worst case scenario, can be up to 8K for black rhombs (a combination of vibration and libration bands) and up to 12 K for transparent squares (vibration band alone).

[19] The density of ice particles, calculated with the retrieval procedure described by *Zasetsky et al.* [2004] and new ice temperature presented in Figure 5, is shown in Figure 6 as a function of tangent altitude. We note that,

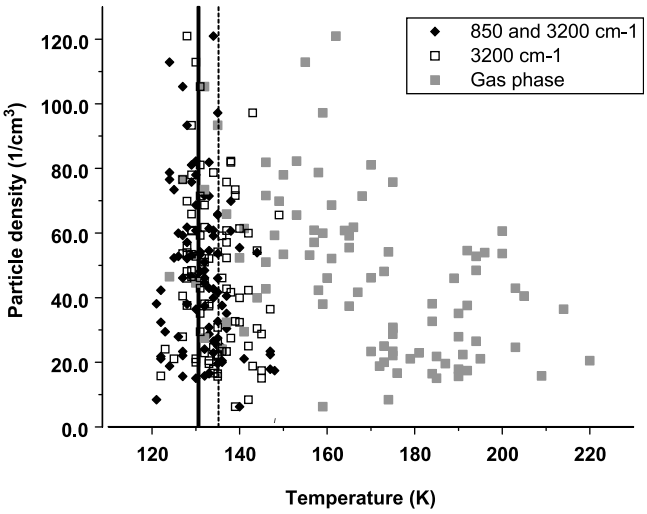

Figure 5. Ice particle number density versus ice temperature retrieved in this work (black rhombs) in comparison to that obtained by *Petelina and Zasetsky* [2009] from the O-H stretch band alone (open squares) and gas phase (CO_2) rotational lines (gray squares). The solid vertical line indicates mean ice temperature retrieved from both 850 cm^{-1} and 3200 cm^{-1} bands, while the dashed vertical line indicates that retrieved from the 3200 cm^{-1} band only.

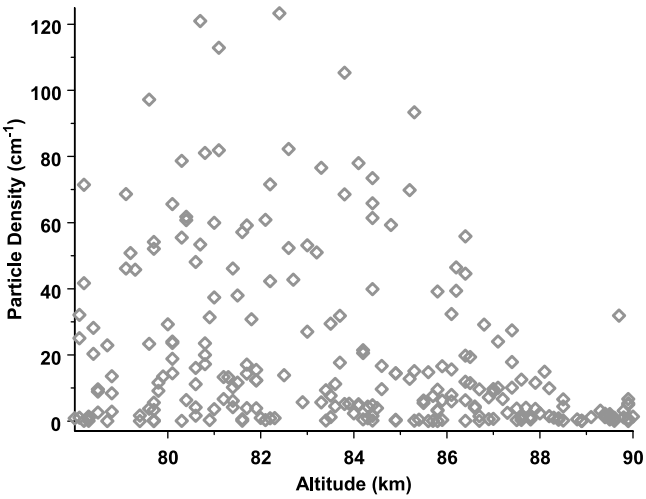

Figure 6. Density of ice particles as a function of their tangent altitude retrieved from the ACE-FTS PMC spectra in July 2005. Diamonds represent individual observations with density retrieved for the thickest layer in a PMC profile.

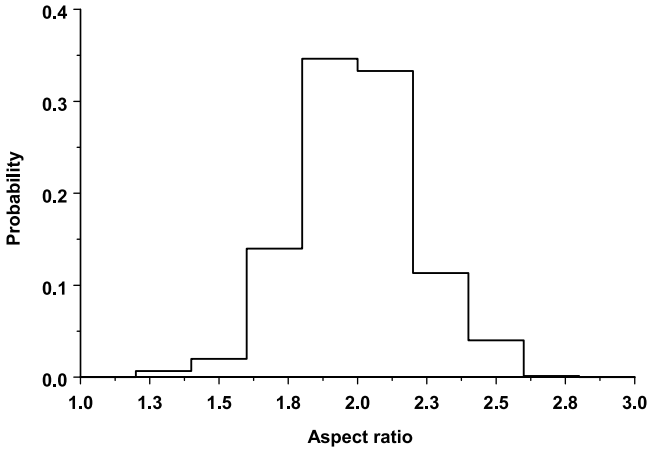

Figure 7. Probability distribution for the retrieved ice particles axial ratio values when particles are treated as randomly oriented oblate spheroids.

same as in our earlier work [*Petelina and Zasetsky*, 2009], the ice volume density has been calculated first, but then converted into the ice particle density for illustration purposes. The latter values are determined from the ice mass density under the assumption that particles have an effective radius of about 60 nm. As was described in our early publications [e.g., *Zasetsky et al.*, 2009a; *Zasetsky et al.*, 2009b; *Petelina and Zasetsky*, 2009], the ACE-FTS infrared spectra are sensitive to the volume of ice (or ice mass density), but not to the variations in the size of ice particles within the 10–100 nm range. Therefore, our assumption on the particle effective radius of 60 nm, based on the coincident data measured by a different satellite instrument as described by *Eremenko et al.* [2005], does not affect the results presented in this work. We also note that the contribution of ice particles with radius < 10 nm to the total volume is small and therefore can hardly be detected by ACE-FTS (this is a threshold of ACE-FTS ice delectability) and thus are not accounted for in this study.

[20] The vertical distribution of the ice particle number density shown in Figure 6 is somewhat nonuniform, but in general the density increases with decreasing altitude. However, this increase in density with decreasing altitude is not as prominent compared to some other recent studies [e.g., *Hervig et al.*, 2009a]. We attribute this fact to a wider field of view of the ACE-FTS instrument that does not allow for high enough vertical resolution of the observed PMCs. At the same time, the ice number density at altitudes above 87 km, where the nucleation of ice particles typically occurs, is about 4 times smaller than that at 81 km. This is in good agreement with the results of modeling and remote sensing observations [e.g., *Rapp and Thomas*, 2006; *von Zahn and Berger*, 2003; *Hervig et al.*, 2009a]. The ice number density maximizes near 81 km, which agrees well with simulations and observations. As the temperature at the altitudes between 80 and 82 km in the summer polar mesosphere is often higher than the ice freezing point, ice particles evaporate quickly and are rarely seen below 80 km [e.g., *Lübken*, 1999; *Rapp and Thomas*, 2006; *Feofilov and Petelina*, 2010]. It should be noted that due to the 4 km wide field of view, and also because clouds in the near and far field of view tend to appear to reside lower than they actually are, PMCs observed by the ACE-FTS instrument below 80 km are excluded from the present analysis.

[21] The distribution of axial ratio (AR) values for oblate spheroids, which are commonly used to represent ice crystals, is shown in Figure 7. These AR values for ACE-FTS PMCs are determined simultaneously with the new ice particle temperature. This is done using the same method as described by *Hervig and Gordley* [2010], and our results are in a good agreement with the SOFIE results. We found that, on average, the AR of 1.9 is best suited to model the ACE-FTS extinction spectra of ice particles in the mesosphere. Note that in contrast to *Hervig and Gordley* [2010], we were not able to differentiate the AR values over tangent heights or temperatures because of relatively small number of the measurements analyzed.

4. Concluding Remarks

[22] An improved technique for the retrieval of the temperature of ice particles formed in the Earth's upper mesosphere is described in this work. A combination of the libration 850 cm^{-1} band and the vibration 3200 cm^{-1} band in the spectrum of water ice is used. The technique is applied to ~100 PMC observations made by the ACE-FTS satellite instrument in July 2005. The estimated total uncertainty in the temperature retrievals with this new method is found to be 8K, or less, and is reduced by about 4–5K as compared to the results obtained using the 3200 cm^{-1} band alone.

[23] The mean ice temperature of 131K in July 2005 retrieved in this work agrees well with the value of 131–132K observed in July 2008 by the SOFIE instrument below 86 km [see *Hervig and Gordley*, 2010, Figure 6a]. We focus on this altitude range in SOFIE observations because only bright ACE-FTS PMCs are used in this work, and it is well known that bright clouds tend to be at lower altitudes. Although SOFIE retrievals are not based on a simultaneous analysis of the O-H stretch and libration bands, the quality of their measurements and retrievals are high, with the reported uncertainty on the order of 9K or less. By adding the 850 cm^{-1} libration band to the analysis of ACE-FTS data, we have reduced the uncertainty of 12K in the retrieved ice temperature values earlier reported earlier by *Petelina and Zasetsky* [2009] to 8K, or less, which is comparable to that of SOFIE. This makes the ACE-FTS long-term (2004 to present) data set on PMC events in both hemispheres even more important and potentially interesting for studying interseasonal and interhemispheric variability and trends in mesospheric properties. Such analysis is not a part of the present study, but is planned to be carried out in the near future.

[24] The present study has exposed once more a crucial role played by experimental optical constants and a strong need for a consistent set of accurate optical constants for water ice in the frequency range of 400 to 5000 cm^{-1} and the temperature range from 120 to 200K. The uncertainty in experimental optical constants may contribute more than 50% to the total uncertainty of the retrieved ice temperatures. If the exact values for these constants were known, the ice

temperature uncertainty would be reduced down to 4–6 K (depending on the brightness of individual PMCs). Another way to reduce the ice temperature retrieval errors is to increase the signal-to-noise ratio in the low-frequency region < 1000 cm^{-1}, together with the extension of infrared observations down to 400 cm^{-1}. In summary, combining IR measurements in the vicinity O-H stretch band (3200 cm^{-1}), which puts tight constraints on the particle shape, with *low noise* measurements near H_2O libration band (850 cm^{-1}), which is sensitive to temperature due to its rotational nature, may reduce the statistical (fitting) error in ice temperature retrievals to 2–4 K.

[25] **Acknowledgments.** Part of this work was supported by the Australian Research Council, Discovery Project DP1096960. The Atmospheric Chemistry Experiment (ACE) is a Canadian-led mission mainly funded by the Canadian Space Agency. ACE is also currently supported by the European Space Agency as a third-party mission.

References

Bernath, P. F., et al. (2005), Atmospheric Chemistry Experiment (ACE): Mission overview, *Geophys. Res. Lett.*, *32*, L15S01, doi:10.1029/2005GL022386.

Bertie, J. E., H. J. Labbe, and E. J. Whalley (1969), Absorptivity of ice I in the range 4000–30 cm^{-1}, *J. Chem. Phys.*, *50*, 4501–4519, doi:10.1063/1.1670922.

Bohren, G., and D. Huffman (1983), *Absorption and Scattering of Light by Small Particles*, 365 pp., John Wiley, Hoboken, N. J.

Boone, C. D., et al. (2005), Retrievals for the atmospheric chemistry experiment Fourier-transform spectrometer, *Appl. Opt.*, *44*, 7218–7231, doi:10.1364/AO.44.007218.

Clapp, M. L., R. E. Miller, and D. R. Worsnop (1995), Frequency-dependent optical-constants of water ice obtained directly from aerosol extinction spectra, *J. Phys. Chem.*, *99*, 6317–6326, doi:10.1021/j100017a010.

Eremenko, M. N., et al. (2005), Shape and composition of PMC particles derived from satellite remote sensing measurements, *Geophys. Res. Lett.*, *32*, L16S06, doi:10.1029/2005GL023013.

Espy, P. J., and H. Jutta (2002), Equilibrium temperature of water0ice aerosols in the high-latitude summer mesosphere, *J. Atmos. Sol. Terr. Phys.*, *64*, 1823–1832, doi:10.1016/S1364-6826(02)00191-8.

Feofilov, A. G., and S. V. Petelina (2010), Relation between mesospheric ice clouds, temperature and water vapor determined from Odin/OSIRIS and TIMED/SABER data, *J. Geophys. Res.*, *115*, D18305, doi:10.1029/2009JD013619.

Gerding, M., J. Höffner, M. Rauthe, W. Singer, M. Zecha, and F.-J. Lübken (2007), Simultaneous observation of noctilucent clouds, mesospheric summer echoes, and temperature at a midlatitude station (54°N), *J. Geophys. Res.*, *112*, D12111, doi:10.1029/2006JD008135.

Hansen, G., and U. von Zahn (1994), Simultaneous observations of noctilucent clouds and mesopause temperatures by lidar, *J. Geophys. Res.*, *99*(D9), 18,989–18,999, doi:10.1029/94JD01524.

Hervig, M. E., and L. L. Gordley (2010), Temperature, shape, and phase of mesospheric ice from Solar Occultation for Ice Experiment observations, *J. Geophys. Res.*, *115*, D15208, doi:10.1029/2010JD013918.

Hervig, M., and D. Siskind (2006), Decadal and inter-hemispheric variability in polar mesospheric clouds, water vapor, and temperature, *J. Atmos. Sol. Terr. Phys.*, *68*, 30–41, doi:10.1016/j.jastp.2005.08.010.

Hervig, M. E., L. L. Gordley, J. M. Russell III, and S. M. Bailey (2009a), SOFIE PMC observations during the northern summer of 2007, *J. Atmos. Sol. Terr. Phys.*, *71*, 331–339, doi:10.1016/j.jastp.2008.08.010.

Hervig, M. E., M. H. Stevens, L. L. Gordley, L. E. Deaver, J. M. Russell, and S. Bailey (2009b), Relationships between PMCs, temperature and water vapor from SOFIE observations, *J. Geophys. Res.*, *114*, D20203, doi:10.1029/2009JD012302.

Lübken, F.-J. (1999), Thermal structure of the Arctic summer mesosphere, *J. Geophys. Res.*, *104*(D8), 9135–9149, doi:10.1029/1999JD900076.

Lübken, F.-J., M. Rapp, and I. Strelnikova (2007), The sensitivity of mesospheric ice layers to atmospheric background temperatures and water vapor, *Adv. Space Res.*, *40*, 794–801, doi:10.1016/j.asr.2007.01.014.

Mishchenko, M. I., and L. D. Travis (1998), Capabilities and limitations of a current FORTRAN implementation of the T-matrix method for randomly oriented, rotationally symmetric scatterers, *J. Quant. Spectrosc. Radiat. Transfer*, *60*, 309–324, doi:10.1016/S0022-4073(98)00008-9.

Murray, B. J., and E. J. Jensen (2009), Homogeneous nucleation of amorphous solid water particles in the upper mesosphere, *J. Atmos. Sol. Terr. Phys.*, *72*, 51–61, doi:10.1016/j.jastp.2009.10.007.

Petelina, S. V., and A. Y. Zasetsky (2009), Temperature of mesospheric ice retrieved from the O-H stretch band, *Geophys. Res. Lett.*, *36*, L15804, doi:10.1029/2009GL038488.

Petelina, S. V., D. A. Degenstein, E. J. Llewellyn, N. D. Lloyd, C. J. Mertens, M. G. Mlynczak, and J. M. Russell III (2005), Thermal conditions for PMC existence derived from Odin/OSIRIS and TIMED/SABER data, *Geophys. Res. Lett.*, *32*, L17813, doi:10.1029/2005GL023099.

Purcell, E. M., and C. R. Pennypacker (1973), Scattering and absorption of light by nonspherical dielectric grains, *Astrophys. J.*, *186*, 705–714, doi:10.1086/152538.

Rapp, M., and G. E. Thomas (2006), Modeling the microphysics of mesospheric ice particles: Assessment of current capabilities and basic sensitivities, *J. Atmos. Sol. Terr. Phys.*, *68*, 715–744, doi:10.1016/j.jastp.2005.10.015.

Rapp, M., F.-J. Lübken, A. Müllemann, G. E. Thomas, and E. J. Jensen (2002), Small-scale temperature variations in the vicinity of NLC: Experimental and model results, *J. Geophys. Res.*, *107*(D19), 4392, doi:10.1029/2001JD001241.

Robert, C. E., C. von Savigny, J. P. Burrows, and G. Baumgarten (2009), Climatology of noctilucent cloud radii and occurrence frequency using SCIAMACHY, *J. Atmos. Sol. Terr. Phys.*, *71*, 408–423, doi:10.1016/j.jastp.2008.10.015.

Russell, J. M., III, et al. (2009), The Aeronomy of Ice in the Mesosphere (AIM) mission: Overview and early science results, *J. Atmos. Sol. Terr. Phys.*, *71*, 289–299, doi:10.1016/j.jastp.2008.08.011.

Shettle, E. P., M. T. DeLand, G. E. Thomas, and J. J. Olivero (2009), Long term variations in the frequency of polar mesospheric clouds in the Northern Hemisphere from SBUV, *Geophys. Res. Lett.*, *36*, L02803, doi:10.1029/2008GL036048.

Sica, R. J., et al. (2008), Validation of the Atmospheric Chemistry Experiment (ACE) version 2.2 temperature using ground-based and space-borne measurements, *Atmos. Chem. Phys.*, *8*, 35–62, doi:10.5194/acp-8-35-2008.

Thomas, G. E. (2003), Are noctilucent clouds harbingers of global change in the middle atmosphere?, *Adv. Space Res.*, *32*, 1737–1746, doi:10.1016/S0273-1177(03)90470-4.

Toon, O. B., M. A. Tolbert, B. Koehler, A. M. Middlebrook, and I. Jordan (1994), Infrared optical constants of H_2O ice, amorphous nitric acid solutions, and nitric acid hydrates, *J. Geophys. Res.*, *99*(D12), 25,631–25,654, doi:10.1029/94JD02388.

Urban, J., et al. (2007), Global observations of middle atmospheric water vapor by the Odin satellite: An overview, *Planet. Space Sci.*, *55*, 1093–1102, doi:10.1016/j.pss.2006.11.021.

von Savigny, C., M. Sinnhuber, H. Bovensmann, J. P. Burrows, M.-B. Kallenrode, and M. Schwartz (2007), On the disappearance of noctilucent clouds during the January 2005 solar proton events, *Geophys. Res. Lett.*, *34*, L02805, doi:10.1029/2006GL028106.

von Zahn, U., and U. Berger (2003), Persistent ice cloud in the midsummer upper mesosphere at high latitudes: Three-dimensional modeling and cloud interactions with ambient water vapor, *J. Geophys. Res.*, *108*(D8), 8451, doi:10.1029/2002JD002409.

Wagner, R., C. Linke, K.-H. Naumann, M. Schnaiter, M. Vragel, M. Gangl, and H. Horvath (2009), A review of optical measurements at the aerosol and cloud chamber AIDA, *J. Quant. Spectrosc. Radiat. Transfer*, *110*, 930–949, doi:10.1016/j.jqsrt.2009.01.026.

Warren, S. G. (1984), Optical constants of ice from the ultraviolet to the microwave, *Appl. Opt.*, *23*, 1206–1225, doi:10.1364/AO.23.001206.

Warren, S. G., and R. E. Brandt (2008), Optical constants of ice from the ultraviolet to the microwave: A revised compilation, *J. Geophys. Res.*, *113*, D14220, doi:10.1029/2007JD009744.

Zasetsky, A. Y., and V. I. Gaiduk (2007), Study of temperature effect on far infrared spectra of liquid H_2O and D_2O by analytical theory and molecular dynamic simulation, *J. Phys. Chem. A*, *111*, 5599–5606, doi:10.1021/jp0717903.

Zasetsky, A. Y., A. F. Khalizov, and J. J. Sloan (2004), Characterization of atmospheric aerosols from infrared measurements: Simulations, testing, and applications, *Appl. Opt.*, *43*, 5503–5511, doi:10.1364/AO.43.005503.

Zasetsky, A. Y., A. F. Khalizov, M. E. Earle, and J. J. Sloan (2005), Frequency dependent complex refractive indices of supercooled liquid water and ice determined from aerosol extinction spectra, *J. Phys. Chem. A*, *109*, 2760–2764, doi:10.1021/jp044823c.

Zasetsky, A. Y., et al. (2007), Retrieval of aerosol physical and chemical properties from mid-infrared extinction spectra, *J. Quant. Spectrosc. Radiat. Transfer*, *107*, 294–305, doi:10.1016/j.jqsrt.2007.02.016.

Zasetsky, A. Y., S. V. Petelina, and I. M. Svishchev (2009a), Thermodynamics of homogeneous nucleation of ice particles in the polar summer mesosphere, *Atmos. Chem. Phys.*, *9*, 965–971, doi:10.5194/acp-9-965-2009.

Zasetsky, A. Y., S. V. Petelina, R. Remorov, C. D. Boone, P. F. Bernath, and E. J. Llewellyn (2009b), Ice particle growth in the polar summer mesosphere: Formation time and equilibrium size, *Geophys. Res. Lett.*, *36*, L15803, doi:10.1029/2009GL038727.

S. V. Petelina, Department of Physics, La Trobe University, Melbourne, VIC 3086, Australia. (s.petelina@latrobe.edu.au)

A. Y. Zasetsky, Department of Radio and Electrical Engineering, Moscow State Technical University, 2-nd Baumanskaya, 5, Moscow 105005, Russia.